Discrete EquiSpaced Unshaded Line Array method for target identification using side scan sonar imagery

M Z Lubis[1*], W Anurogo[1], H Kausarian[2], T Choanji[2], S Antoni[3], S Pujiyati[4]

[1] Geomatics Engineering, Politeknik Negeri Batam, Batam 29461, Indonesia
[2] Faculty of Engineering, Universitas Islam Riau, Pekanbaru, 28284, Indonesia
[3] Marine Geology Department, King Abdulaziz University, Jeddah. Saudi Arabia
[4] Department of Marine Science and Technology, Institut Pertanian Bogor, Indonesia
*e-mail: zainuddinlubis@polibatam.ac.id

Abstract. Beam pattern resulting from Discrete Equispaced Unshaded Line Array method is to analyze the pattern of two-dimensional beam pivot at the angle of sound waves coming from the direction of origin on the axis of the received array, will affect the sound beam angle. This research was conducted in December 2016 in the Punggur Sea, Batam, Riau Islands-Indonesia, and its coordinate system is 104° 08.7102 E and 1° 03.2448 N until 1° 03.3977 N and 104° 08.8133 E, DEULA method in target 4 has the highest value in the directivity pattern is 21.08 dB. The results of the beam pattern model show that neither the central value at the incidence angle (º) of the directivity pattern (dB) were not at the 0 (zero) or the beam pattern central have been generated by the target 6 with incident angle -1.5º and 1.5º. In addition, it has declined by 40 dB. Highest result of line trace is target 1 with 191, 88 cm on target 1, and highest of time result is 13568 cm/second on target 4. Seismic figure of side scan sonar imagery have total line trace is 4479, time: 77.9547 cm/s, and gain: 0.00271091.

1. Introduction

Punggur Sea is the part of the Riau Islands in Indonesia. Generally Punggur Sea still rarely done research on the identification of seabed using the acoustic wave technology. Worldwide, these marine environments have not been studied using high-resolution hydro-acoustic methods (eg, bathymetry, and base profiles), useful for investigation of sediment processes, benthic habitats, mineral resources, artificial artifacts, and other features. Side-scan sonar imagery and underwater photography, coupled with bathymetric and sedimentology data, revealed noteworthy features and the interplay of multiple processes on the Riau Island and Punggur Sea, Indonesia [1]. The seafloor imagery, target identification, and image processing with two dimensional was conducted on the Punggur Sea in 2017 [1, 2].

The side scan sonar (SSS) instrument is a sonar development that able to observe and show the two-dimensional surface pictures by the counter of the sea floor, topography, and the target simultaneously. This instrument is able to distinguish the small particles of the seabed structure such as rocks, muds, sand, gravel, or basic types other waters [3]. Side-scan sonar is an active sonar system which implemented the characteristics of sideways look, two channels, narrow beam, and towed body [4, 5]. The passive acoustic monitoring method with species-specific transmission beam pattern influences the facility with which animals can be localized by a hydrophone array [6].

The principle of a side scan sonar can be seen in figure 1, and the system resolution: governed by the shape of the acoustic beam and the length of the transmitted pulse [7, 8]. So it depends on the three-dimensional distribution of the acoustic energy of the system that affects the size of the footprint. If the

side-scan sonar has low frequency sources (10-30 kHz), the sound pulse will be transmitted and received at long range (covering a large area in a short time) [9, 10]. More particularly, the application of the system is wide-ranging in marine geology, marine biology, hydrography, underwater archaeology, oceanic engineering, and surveys for military purposes [11]. Regarding the monitoring technologies of benthic artificial habitats, the side-scan sonar system has been proposed as the most practical [12]. However, due to the cost of the system, the complexities of its operation procedures, the necessities of a precise track chart for the ship, and extensive period of time and experience for data processing.

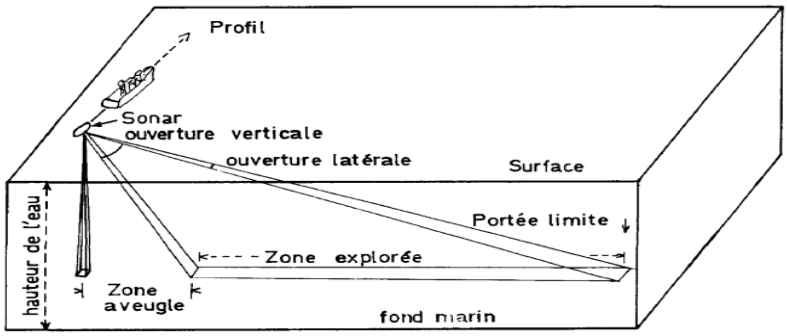

Figure 1. Principle of a side scan sonar [1].

2. Methods

2.1. Study area

This research was conducted in December 2016 at the Punggur Sea, Batam, Riau Islands, Indonesia at the coordinate of 104°08.7102 E and 1° to 1° N 03.2448 03.3977 08.8133 N and 104° E . This research has 3 tracks (figure 2). Acoustic data acquisition was done using a Side Scan C-Max CM2 sonar tow fish instrument also it was set at a frequency of 325 kHz with performs a seabed mapping process that will get features down with two frequency (Port and starboard) display appearance, and a maximum distance of 200 m and 25 m cable length, and a maximum distance of 200 m and 25 m cable length, this study location can be seen in figure 2.

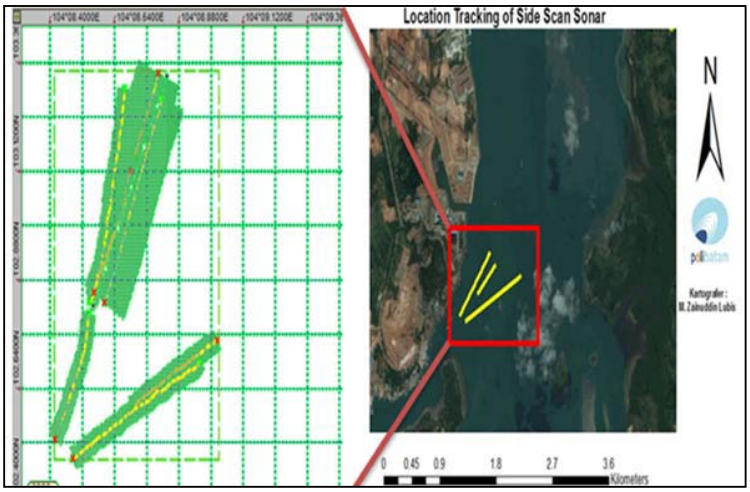

Figure 2.The location of the side scan sonar recording and its observation (3 line of the survey to collecting data in Punggur Sea with the seen on yellow line).

2.2. Two-dimensional beam pattern

The characteristics of beam pattern C-Max CM2 of Side Scan Sonar Tow Fish can be seen in figure 3.

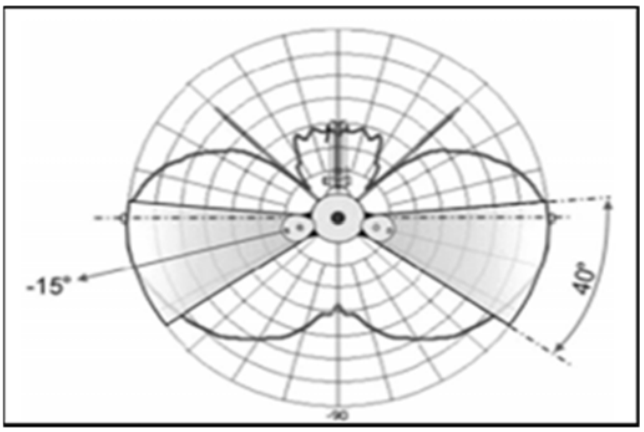

Figure 3. The beam pattern C-Max CM2 of Side Scan Sonar Tow Fish characteristic [5].

Calculating the two-dimensional beam pattern depends on the angle of the incoming sound waves from the array axis, the received power depends on the angle at which light sound incident to array. We can describe this angular dependence with an equation to relate the actual strength that was accepted for the average time power to the shaft (where, θ = 0° and the maximum power is a). The Beam Pattern Discrete-Equispaced Unshaded Line Array can be seen in (figure 4). This ratio is a function of beam pattern two-dimensional array, b (θ) [4] where:

$$b(\theta) = \frac{(P(\theta))}{(P(\theta=0°))} = \frac{\frac{(M_{P_{max}})^2}{R}(1+ cos\ \delta)}{\frac{(M_{P_{max}})^2}{R}(1+ cos\ 0°)}$$

$$b(\theta) = \frac{\frac{(M_{P_{max}})^2}{R}(1+ cos\ (kd\ sin\theta))}{2\frac{(M_{P_{max}})^2}{R}} = \frac{(1+cos(kd\ sin\theta))}{2} \quad (1)$$

Using a geometric identification in the sonar system:

$$1 + cos\theta = 2\left(cos^2(\frac{\theta}{2})\right)$$

$$b(\theta) = \left[cos^2(\frac{kd\sin\theta}{2})\right]$$

or

$$b(\theta) = \left[cos^2(\frac{\pi d\sin\theta}{\lambda})\right] \quad (2)$$

$$b(\theta) = \left(\frac{V}{2}\right)^2 \quad (3)$$

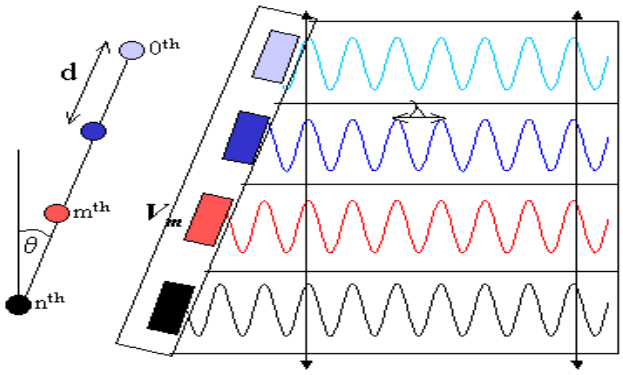

Figure 4. Model the beam pattern, using simple mathematical modeling of Discrete-Equispaced Unshaded Line Array.

3. Results and discussion

Generally, the upper slope of the seafloor will be filled by fine-grained sediments and the bottom will be filled by coarse-grained sediments. Variations of dark and bright colours on the side scan sonar image show the backscattered energy generated from the seafloor. Bright colours will show a high backscatter value whereas dark colours indicate a low backscatter value [22, 23]. It was caused by the gravity force. However, based on the side scan sonar image can be seen the differences between the texture and roughness clearly on the sediments of sand, biogenic sand and mud. There are 7 targets were detected by recording the image of Side Scan Sonar used C-MAX with an estimation of target detection could be observed the large object by the visual images on the target 6 at coordinates 1° 03.3977 N and 104° 08.8133 (figure5). These objects can be indicated was a sunken wreck on the seabed of Punggur Sea, Batam, Riau Islands, Indonesia. The result of the time acquisition, ping position, gain and elevation of the SSS recording can be seen in figure 1. In addition, figure 5 shows the image result of the seabed.

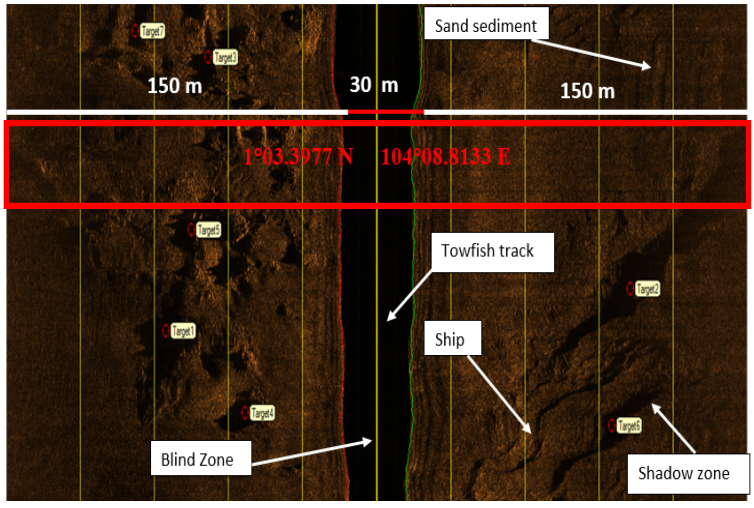

Figure 5. The classification of the seafloor sediments in the Punggur Sea.

There are several lines on the sediment image. Its indication was caused by the influence of the boat and tow vehicle movements so that disrupt the appearance of the image (figure 7). The physical characteristic of the Punggur Sea was having the dynamical current sea. This causes movement of the

tow vehicle more difficult to control. Based on data from the movement of side scan sonar was founded the sensor pitch movements until 15 degrees from a standstill 0 degrees roll movements occur up to 10 degrees from its position as well as 0 degrees.

Image of seafloor sediments with the 7 targets. The target of 6 was the object of the sunken ship on the seafloor, while sand object can be seen clearly (figure 6), while the other targets (target 1-5 and target 7) do not indicate the object of the sinking vessel, but the seabed in the form of sand and rough sediment on the seabed. The ship object was founded at the coordinate of 1°03.3101 N and 104°08.7362 E. On the port (right side) was seen the lighter entrenchment. Their excavation led to differences in texture, roughness and slope of the seafloor sediments. Furthermore, the excavation that occurred on the seabed was indicated causing the larger particle sediments was lifted up.

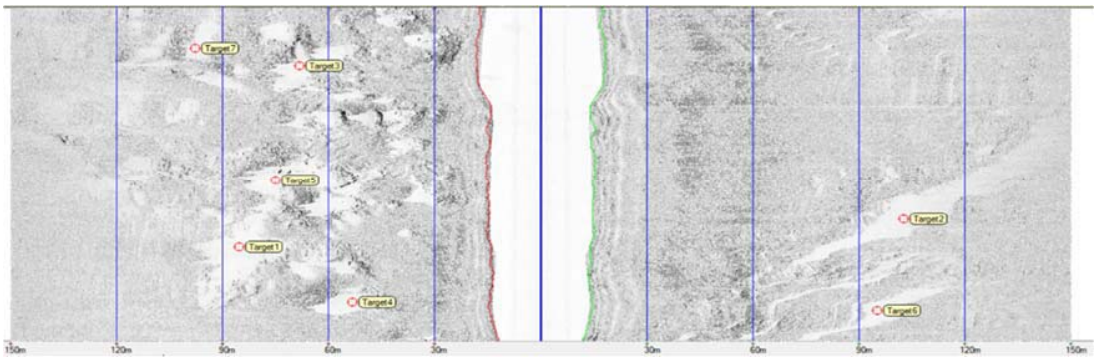

Figure 6. Image of seafloor sediments with the 7 targets.

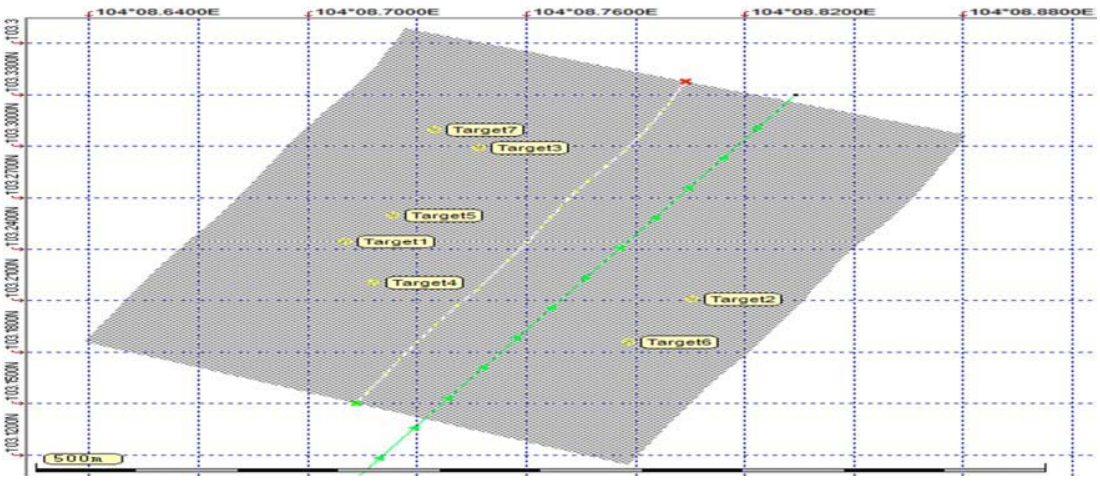

Figure 7. The target positions and the seafloor image by SSS tracking.

According to the results of visual detection [13, 14] grain size, sediment surface roughness scale and significant slope variations could be important role in the acoustic response. The swift currents would precipitate coarse grain sediments and the weak current would precipitate the fine-grained sediments. However, the seafloor condition will affect the location of the sediment. According to [15, 16] a sweep of side scan sonar can produce mosaics, geological and sedimentology features that are easily to observe and interpreted qualitatively so could provide the information about the dynamics of the ocean floor.

The beam pattern incidence angle (°) of the directivity pattern (dB) and beam pattern can be seen in figure 8.

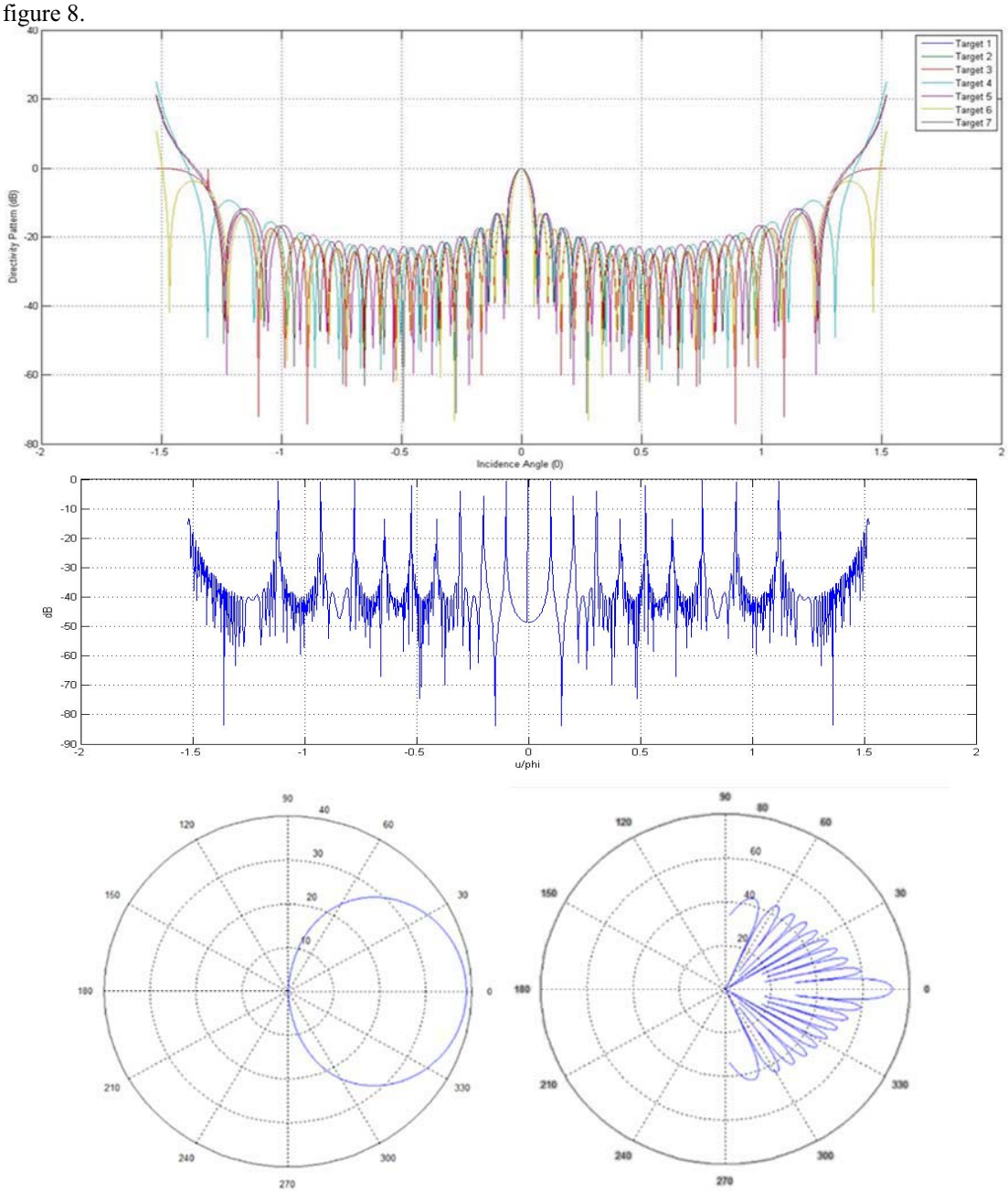

Figure 8. The beam pattern incidence angle (°) of the directivity pattern (dB) and Beam pattern (the results are obtained from the processing of data frequency, altitude and power generated on the side scan sonar (SSS) data on MATLAB software.

The target amount as well as 7 targets on Beam pattern of Discrete Equispaced Line Array unshaded method, the target of 4 has the highest value at 21.08 dB of its directivity Pattern was shown in light blue. By looking at the centre of the model beam pattern result, the target of 6 has a central value of the

incidence angle (°) of the directivity pattern (dB) are not in a value of 0 or at the centre of the resulting beam pattern. On target of 6 there is a value of incident angle -1.5° and 1.5° has decreased to -40 dB. This relation can be seen to the value of altitude (m) which is 18.1m and a gain of 6 dB which allegedly was the object of the shipwreck on the seabed. On the target of 4 has the values of incident angle -1.32° and 1.32° and also decreased up to -50 dB. The de-convolution of this method result shows the beam pattern which was still concentrated by touching the second quadrant of the existing signal, these results provide a similar pattern the beam and a beam generated by looking at the value of the wavelength and frequency is generated [17-18]. This can be seen in relation to the value of altitude (m) which is worth 17.8 and gain value of 5 dB which is the object of the shipwreck on the seabed allegedly.

Seismic line trace of target detection have 41 number of data collection from side scan sonar imagery after processing (is the result of extraction of side scan feature (.xtf into SEG-Y file). Highest of seismic line trace of target detection is target 3 with 1664 (figure 9).

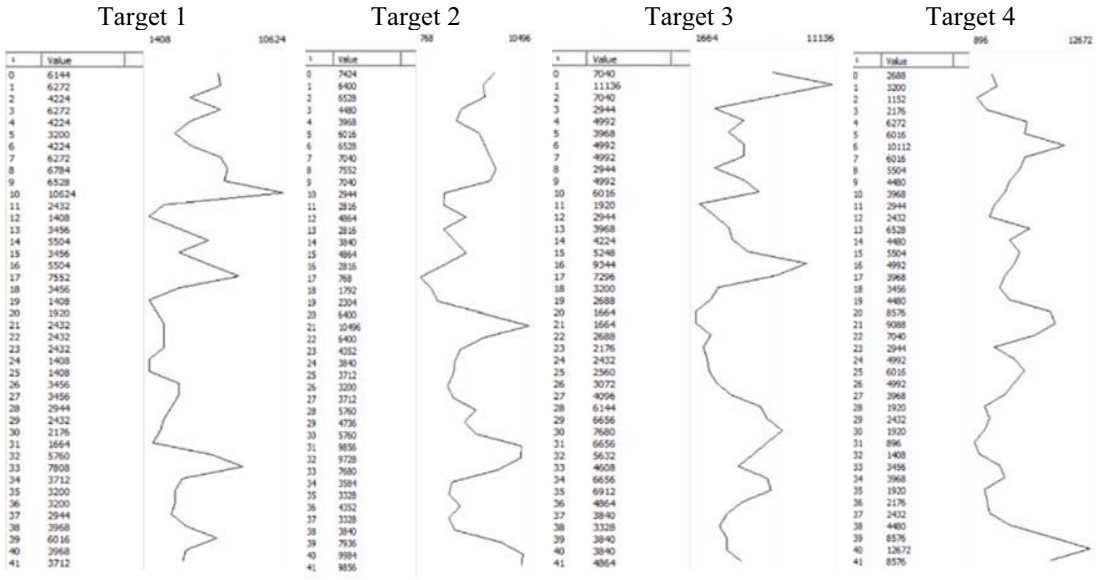

Figure 9. Seismic line trace of target detection.

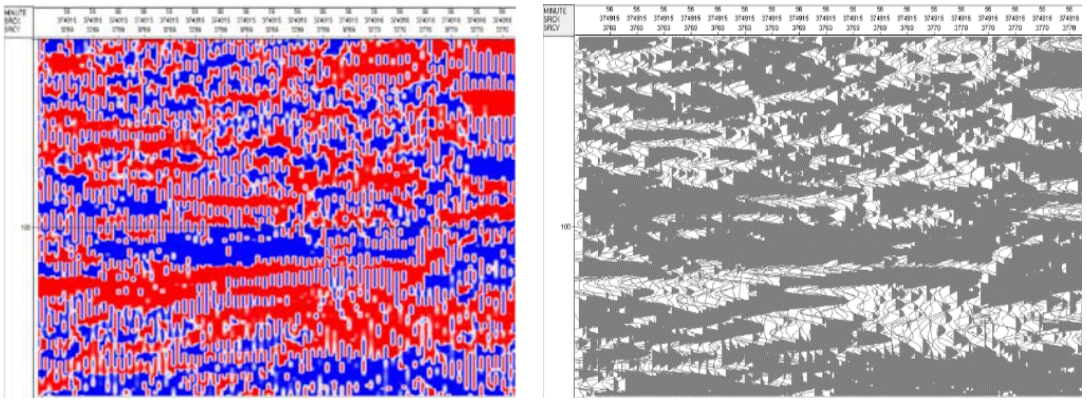

Figure 10. 2D seismic cross-section from side scan sonar (SSS) data extraction results.

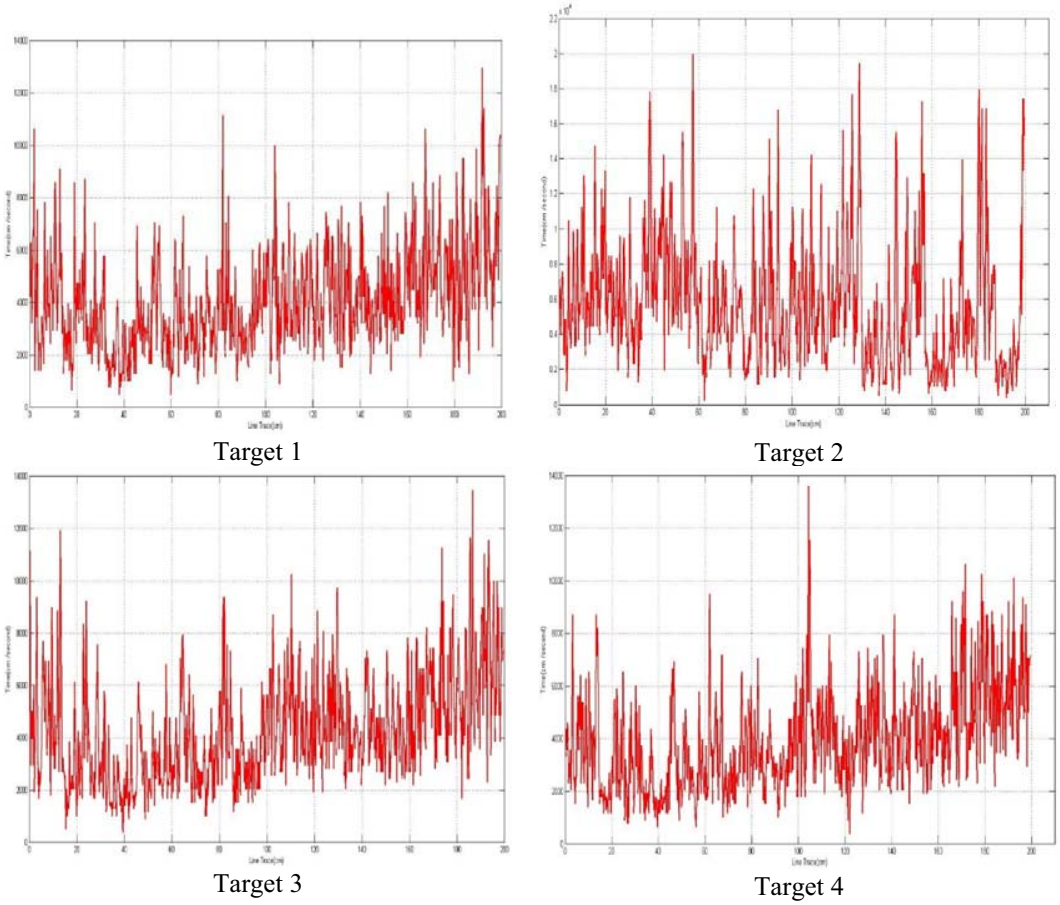

Figure 11. Line trace (cm) vs time (cm/second) target 1-4.

Identification of seismic line trace with identification target must be important for seismic investigation and analysis [19, 21]. Line trace (cm) vs time (cm/second) target 1-4 has obtained from the data extraction using MaxView software that is exported to .txt, by generating time data. While the data line trace is the process of data processing resulting from 2D cross-sectional data (figure 10) Figure of line trace vs time have max data is 200 on line trace and 220 x 103 time in target 2. Highest result of the time in figure 9 is 12928 cm/second and 191, 88 cm in line trace target 1 of side scan sonar imagery. The highest result in figure 7 with the value 9968 cm/second and 57, 525 cm in line trace target 2 of side scan sonar imagery. The highest result in figure 10 with the value 13440 cm/second and 186, 615 cm in line trace target 3 of side scan sonar imagery. Highest result of the time in (figure 11) is 13568 cm/second and 104, 325 cm in line trace target 4 of side scan sonar imagery. Highest result of line trace is target 1 with 191, 88 cm on target 1, and highest of time result is 13568 cm/second on target 4. Seismic figure of side scan sonar imagery have total line trace is 4479, time: 77.9547 cm/s, and gain: 0.00271091 (figure 11).

4. Conclusions

The research in Punggur Sea, Batam using the C-Max CM2 Side Scan Sonar Tow fish at a frequency of 325 kHz, the result of the seabed image is that the more seabed sediment is sand with the target gain and altitude values. The result of the side scan sonar (SSS) image recorded have identified seven targets, while the target of 4 and 6 based on the Discrete-Equispaced Unshaded Line Array method was

discovered the sunken wreck. There is a relationship that has a real relationship between the incident angle (°), directivity pattern (dB), Altitude (m), and a gain value (dB). The Discrete Equispaced unshaded Line Array was a method which can be used to identify the targets on the seabed. The highest result of the line trace was the target 1, and highest of time result on target 4. Target 1 have a relationship with results with highest target detection.

Acknowledgments
We would like to thank the P3M Politeknik Negeri Batam and Geomatics Engineering D3 Programs Politeknik Negeri Batam who helped and guided us so that we have completed our research.

References

[1] Lubis M Z, Anurogo W, Khoirunnisa H, Irawan S, Gustin O and Roziqin A 2017 Using Side-Scan Sonar instrument to characterize and map of seabed identification target in punggur sea of the Riau Islands, Indonesia *Journal of Geoscience, Engineering, Environment, and Technology* **2**(1) 1-8
[2] Lubis M Z, Lubis R A and Lubis R U A 2017 Two-dimensional wavelet transform de-noising and combining with side scan sonar image *Journal of Applied Geospatial Information* **1**(1) 1-4
[3] Bartholomä A 2006 Acoustic bottom detection and seabed classification in the German Bight, Southern North Sea *Geo-Marine Letters* **26**(3) 177
[4] Hamilton L J and Parnum I 2011 Acoustic seabed segmentation from direct statistical clustering of entire multibeam sonar backscatter curves *Continental Shelf Research* **31**(2) 138-148
[5] Bryant R S 2015 Side scan sonar for hydrography-an evaluation by the Canadian Hydrographic Service *The International Hydrographic Review* **52**(1) 43-56
[6] Frey-Martínez J, Cartwright J and James D 2006 Frontally confined versus frontally emergent submarine landslides: a 3D seismic characterisation *Marine and Petroleum Geology* **23**(5) 585-604
[7] Alves T M 2010 3D seismic examples of differential compaction in mass-transport deposits and their effect on post-failure strata *Marine Geology* **271**(3) 212-224
[8] Grothues T M, Newhall A E, Lynch J F, Vogel K S and Gawarkiewicz G G 2016 High-frequency side-scan sonar fish reconnaissance by autonomous underwater vehicles *Canadian Journal of Fisheries and Aquatic Sciences* **74**(2) 240-255
[9] Ruffell A (2014) Lacustrine flow (divers, side scan sonar, hydrogeology, water penetrating radar) used to understand the location of a drowned person *Journal of Hydrology* **513** 164-168
[10] Zhang J, Tao B, Liu H, Jiang W, Gou Z and Wen F 2016 A mosaic method based on feature matching for side scan sonar images *In Ocean Acoustics* (*COA*) IEEE/OES China pp 1-6
[11] Lubis M Z, Taki H M, Anurogo W, Pamungkas D S, Wicaksono P and Aprilliyanti T 2017 Mapping the Distribution of Potential Land Drought in Batam Island Using the Integration of Remote Sensing and Geographic Information Systems (GIS) *IOP Conf. Series: Earth and Environmental Science* IOP Publishing **98**(1) p 012012
[12] Garner J T, Buntin M L, Fobian T B, Holifield J T, Tarpley T A and Johnson P D 2016 Use of side-scan sonar to locate *Tulotoma magnifica* (Conrad, 1834) (Gastropoda: Viviparidae) in the Alabama River *Freshwater Mollusca Biology and Conservation* **19** 51-55
[13] Bond L J, Kepler W F and Frangopol D M 2000 Improved assessment of mass concrete dams using acoustic travel time tomography Part I—theory *Construction and Building Materials* **14**(3) 133-146
[14] Kenny A J, Cato I, Desprez M, Fader G, Schüttenhelm R T E and Side J 2003 An overview of seabed-mapping technologies in the context of marine habitat classification *ICES Journal of Marine Science* **60**(2) 411-418
[15] Taki H M and Lubis M Z 2018 Signal detection for identification energy and behaviour of male dolphin bottle nose (Tursiopsaduncus) using NTD Model *IOP Conf. Series: Earth and Environmental Science* IOP Publishing January **105(**1) p 012029

[16] Owen M J, Maslin M A, Day S J and Long D 2015 Testing the reliability of paper seismic record to SEGY conversion on the surface and shallow sub-surface geology of The Barra Fan (NE Atlantic Ocean) *Marine and Petroleum Geology* **61** 69-81
[17] Singh A, Modi M H, Sinha A K, Dhawan R and Lodha G S 2015 Study of structural and optical properties of zirconium carbide (ZrC) thin-films deposited by ion beam sputtering for soft x-ray optical applications *Surface and Coatings Technology* **272** 409-414
[18] Zhang Y, Wang Y, Li W, Huang Y and Yang J 2015 Scanning radar angular superresolution with fast standard Capon beamformer *In Geoscience and Remote Sensing Symposium* (*IGARSS*) *IEEE International* 2015 pp 3111-3114
[19] Pauselli C, Barchi M R, Federico C, Magnani M B and Minelli G 2006 The crustal structure of The Northern Apennines (central Italy): an insight by the CROP03 seismic line *American Journal of Science* **306**(6) 428-450
[20] Russell B, Hampson D, Schuelke J and Quirein J 1997 Multiattribute seismic analysis *The Leading Edge* **16**(10) 1439-1444
[21] Lagomarsino S and Giovinazzi S 2006 Macroseismic and mechanical models for the vulnerability and damage assessment of current buildings *Bulletin of Earthquake Engineering* **4**(4) 415-443
[22] Chavez P S, Isbrecht J, Galanis P, Gabel G L, Sides S C, Soltesz D L, *et al.* 2002 Processing, mosaicking and management of the Monterey Bay digital sidescan-sonar images *Marine Geology* **181**(1) 305-315
[23] Chang Y C, Hsu S K and Tsai C H 2010 Sidescan sonar image processing: correcting brightness variation and patching gaps *Journal of Marine Science and Technology* **18**(6) 785-789